BMES BIOMEDICAL ENGINEERING SOCIETY

Original Article

Navigation of Microrobots by MRI: Impact of Gravitational, Friction and Thrust Forces on Steering Success

Cyril Tous,[1,2] Ning Li,[1,2] Ivan P. Dimov,[1] Samuel Kadoury,[4]
An Tang,[1,2] Urs O. Häfeli,[5] Zeynab Nosrati,[5] Katayoun Saatchi,[5]
Gerald Moran,[6] Marcus J. Couch,[6] Sylvain Martel,[4]
Simon Lessard,[2,3]
and Gilles Soulez [1,2]

[1]Centre de recherche du Centre hospitalier de l, Université de Montréal (CRCHUM), 900 Rue Saint-Denis, Montreal, QC H2X 0A9, Canada; [2]Université de Montréal, 2900 Boulevard Édouard-Montpetit, Montreal, QC H3T 1J4, Canada; [3]École de Technologie Supérieur, 1100 Rue Notre-Dame O, Montreal, QC H3C 1K3, Canada; [4]Polytechnique Montréal, 2500 Chemin de Polytechnique, 28, Montreal, QC H3T 1J4, Canada; [5]University of British Columbia, 2405 Westbrook Mall, Vancouver, BC V6T 1Z3, Canada; and [6]Siemens Healthineers, Erlangen, Canada

Associate Editor Stefan M Duma oversaw the review of this article.

Abstract—Introduction Magnetic resonance navigation (MRN) uses MRI gradients to steer magnetic drug-eluting beads (MDEBs) across vascular bifurcations. We aim to experimentally verify our theoretical forces balance model (gravitational, thrust, friction, buoyant and gradient steering forces) to improve the MRN targeted success rate. **Method** A single-bifurcation phantom (3 mm inner diameter) made of poly-vinyl alcohol was connected to a cardiac pump at 0.8 mL/s, 60 beats/minutes with a glycerol solution to reproduce the viscosity of blood. MDEB aggregates (25 ± 6 particles, 200 μm) were released into the main branch through a 5F catheter. The phantom was tilted horizontally from − 10 to + 25 to evaluate the MRN performance. **Results** The gravitational force was equivalent to 71.85 mT/m in a 3T MRI. The gradient duration and amplitude had a power relationship (amplitude = 78.717 $(duration)^{-0.525}$). It was possible, in 15 elevated vascular branches, to steer 87% of injected aggregates if two MRI gradients are simultaneously activated ($G_x = +26.5$ mT/m, $G_y = +18$ mT/m for 57% duty cycle), the flow velocity was minimized to 8 cm/s and a residual pulsatile flow to minimize the force of friction. **Conclusion** Our experimental model can determine the maximum elevation angle MRN can perform in a single-bifurcation phantom simulating *in vivo* conditions.

Keywords—MRI duty cycle, Bifurcation phantom, Magnetic drug-eluting beads, Microrobots, Steering aggregate.

Address correspondence to Gilles Soulez, Centre de recherche du Centre hospitalier de l, Université de Montréal (CRCHUM), 900 Rue Saint-Denis, Montreal, QC H2X 0A9, Canada. Electronic mail: gilles.soulez.med@ssss.gouv.qc.ca
Cyril Tous and Ning Li are co-first authors and they have contributed equally to this study article.

ABBREVIATIONS

$\overrightarrow{B0}$	Main MRI magnetic field strength
EPI	Echo planar readout
MDEBs	Magnetic drug-eluting beads
MRN	Magnetic resonance navigation
MRI	Magnetic resonance imaging
PLGA	Poly-lactic-co-glycolic acid
PVA	Poly-vinyl alcohol
T2	Relaxation time of the transverse magnetization
TE	Echo time
TR	Repetition time

INTRODUCTION

Intra arterial chemotherapy, chemo-embolization, prevention of stroke or treatment of vascular disease are all parts of interventional radiology applications based on the endovascular navigation of catheters and guidewires to the therapeutic target. However, superselective catheterization is dependent on the skills and experience of the interventional radiologist. Often, tortuous vessels and friction of the guidewire prevent from reaching the targeted area, leading to incomplete

treatment and frequent reinterventions, adding significant cost on patient care.[9] Therapeutic targeting at a location of interest to concentrate magnetized microrobots[27], magnetotactic bacteria[19] and deviate magnetized tip of a guidewire are all techniques that consist of either activating magnetic gradients for steering and imaging, known as Magnetic Resonance Navigation (MRN)[18] or placing adequately large ferromagnetic cores to perform Dipole Field Navigation (DFN),[14] or using existing MRI fringe field to perform Fringe Field Navigation (FFN).[2] Lastly, a closed-loop control of a Helmholtz coil system for actuation of magnetic microrobot swarms was proposed to form and steer aggregates of nanoparticles.[12] Since the magnetic force increases at a cubic rate of the bead's radius[29], a single magnetic microparticle is difficult to steer. Forming aggregate with known numbers of particles was first introduced by Li et al[3] to optimize steering and increase therapeutic loads per bolus, without the need of external coils.

So far, DFN had only been implemented in non-physiological models of vascular tree and can inadvertently trap microrobots to the nearby strong ferromagnetic core (exceeding 300 mT/m).[14] Although rotating magnetic fields provides a greater magnitude of the field to sustain the aggregate uniformity[1], they rely on close strong magnets limiting their application for deep tissues (> 30 cm) and human size bore (~60 cm). Alternatively, FFN relies on moving the patient in the MRI fringe with a robotic arm, which is challenging to implement in clinical MRI rooms. On the other hand, MRN uses existing clinical MRI scanners to image and steer microrobots. At first, MRN research focused on using stronger gradients and making the magnetic drugs eluting beads (MDEBs) more magnetic, while at the same time making the MDEBs more biocompatible and biodegradable.

To apply the MRN technology to liver cancer chemo-embolization procedures, the anti-cancer drug doxorubicin was first co-encapsulated into 50 μm diameter microspheres consisting of graphite-coated FeCo nanoparticles (60%) (diameter = 206 ± 62 nm) and biodegradable polymer poly-lactic-co-glycolic acid (PLGA) (40%).[28] These FeCo-based MDEBs were successfully steered toward the right or left lobe of rabbit livers, using a coil insert delivering a gradient of 288 ± 13 mT/m.[28] To avoid potential cobalt toxicity and to obtain at particle size optimized for drug delivery in human liver, 200 ± 12 μm (coefficient of variation = 6%) microparticles, composed of superparamagnetic biocompatible iron oxide nanoparticles (12 ± 3.6 nm) coated with C_{12}-bisphosphonate and PLGA (50:50 ester terminated; MW 60−100 kDa; IV 0.76−0.94 dL/g, Durect Co., AL, USA) were synthesized in a co-precipitation method.[22] To maximize the steerability of these MDEBs in our study, we focused on taking advantage of influencing forces such as gravity, the magnetic force between particles, thrust, buoyancy and the steering force induced by the MRI gradients, while reducing the effects that can minimize steering efficiency, e.g., friction force and high flow velocity.

Before injection into the blood circulation, MDEBs were gathered into aggregates of 25 ± 6 microparticles with a controlled magnetic trap.[3] Due to the larger scale of the aggregate in the range of 0.5 to 1 mm in relation to $\overrightarrow{B0}$, this method increases the overall magnetic force required for MRN while preserving the microscopic scale of the particles necessary for a therapeutic effect and decreasing the overall injection time compared with single particle injection.[16, 19] Since the MRI gradients affect the entire field, the subsequent aggregate bolus cannot be released until the previous one reaches the target.[17] In this so-called pulsed-bolus injection, a trigger signal sent to the MRI starts the MRN sequence with a delay accounting for the transit time of the aggregate in the catheter and vascular system. The thrust force generated by blood flow will propel the aggregates into the hepatic vasculature. However, the physiological blood flow velocity (30–40 cm/s) was too high to be compatible with MRN. Injection of aggregates through a partially inflated balloon catheter has therefore been proposed to make the flow velocity range compatible with MRN (10 cm/s).[21]

Due to their density (ρ_p = 2.9500g/cm³), MDEB aggregates accumulate at the bottom of the arterial vessel wall. To minimize friction forces, a baseline continuous non-pulsatile injection flow of 0.2 mL/s in the catheter was combined with a peripheral pulsatile flow around the balloon catheter with a frequency of 60 bpm (beats per minute) and an amplitude of 0.4 mL to generate a slow displacement of the aggregate.[17,21] In flat glass phantoms, one with a single and one with a double bifurcation, a 100% success rate was observed to navigate MDEB aggregates across the first bifurcation and between 80 and 100% for the second bifurcation depending on the orientation of $\overrightarrow{B0}$ relative to the main branch direction.[15] Thus, aggregates can be successfully steered to the desired location with standard clinical MRI gradients (≤ 43 mT/m). However, these experiments did not account for *in vivo* flow conditions, the complex geometry of the hepatic vessel tree, the viscosity of blood, and the applied forces as mentioned above.

Phantoms are used to reproduce *in vivo* conditions and verify theoretical models. They can reproduce wall deformations[25,26], mimicking dynamic viscoelasticity and friction resistance of blood vessels[13,24], under
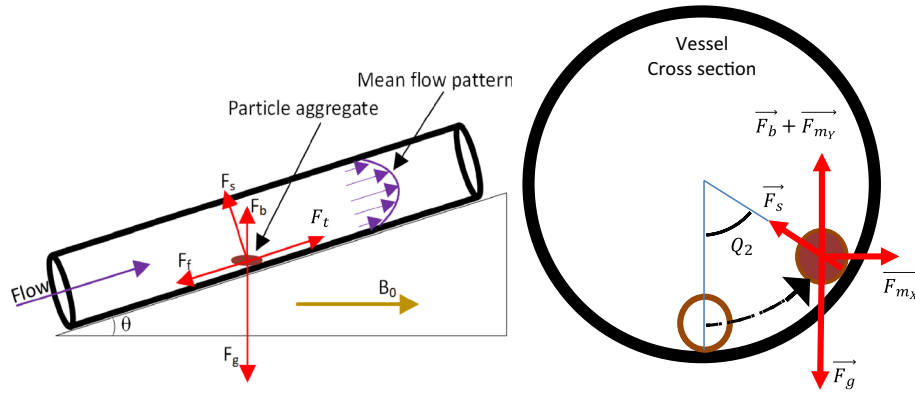
FIGURE 1. Estimation of the thrust force ($\overrightarrow{F_t}$) from the relationship between gravitational force ($\overrightarrow{F_g}$), friction force ($\overrightarrow{F_f}$), supporting force ($\overrightarrow{F_s}$) and buoyancy force ($\overrightarrow{F_b}$), according to the inclination angle (θ), aggregate's speed and flow velocity in a magnetic field ($\overrightarrow{B_0}$). On the right, cross-section of the vessel with the magnetic force ($\overrightarrow{F_m}$) in X and Y direction which levitates the aggregate with an angle (Q_2).

systemic pressure with a cardiac pump. Steering microrobots across multiple bifurcations in phantoms has already been investigated,[7,8,10,15] but disregarded the effect of the gravitational force, the friction force, the curvature of the vessel innerwall, and the pulsatile flow with systemic pressure, all acting on the steering success. They are relevant as a proof of concept but not realistic enough to test *in vivo* feasibility.

In this paper, we are aiming to verify experimentally, our theoretical model of the forces acting on the MDEB aggregate steered by the MRI gradients in realistic *in vivo* flow conditions in a single-bifurcation phantom. We will be able to determine the maximum branch elevation angle which MBEB aggregates can be successfully steered according to the applied MRI gradients and acting forces on the aggregates.

MATERIALS AND METHODS

Theoretical Thrust Force, a Rheologic Model

The aggregate is subject to: the gravity ($\overrightarrow{F_g}$), the thrust force ($\overrightarrow{F_t}$), the friction force ($\overrightarrow{F_f}$), the supporting force ($\overrightarrow{F_s}$) (also known as the normal force), the buoyancy force ($\overrightarrow{F_b}$), the magnetic force ($\overrightarrow{B_0}$), and the magnetic forces from the steering gradients ($\overrightarrow{F_m}$) (Fig. 1).

To achieve the force balance at $\theta = 10°$ without gradient steering, the forces need to satisfy the condition below.

$$\overrightarrow{F_t} - \left(\overrightarrow{F_g} - \overrightarrow{F_b}\right)sin\theta = \mu \bullet \overrightarrow{F_s} \qquad (1.1)$$

Here, $\overrightarrow{F_t}$ and $\overrightarrow{F_s}$ can be expressed by:

$$\|\overrightarrow{F_t}\| = \sigma \cdot (V_{ba} - V_a) \qquad (1.2)$$

$$\overrightarrow{F_s} = \left(\overrightarrow{F_g} - \overrightarrow{F_b}\right)cos\theta \qquad (1.3)$$

where σ is a constant related to the dynamic viscosity of the fluid, and the object size and shape. V_a and V_{ba} are the velocity of the aggregate and the flow velocity bypassing the aggregate, respectively, while μ is the dynamic friction constant. From Equation (1.1)–(1.3):

$$\sigma \cdot (V_{ba} - V_a) - \left(\overrightarrow{F_g} - \overrightarrow{F_b}\right)sin\theta$$
$$= \mu \cdot (\overrightarrow{F_g} - \overrightarrow{F_b})cos\theta \qquad (1.4)$$

For a particle aggregate composed of 200 μm (diameter) particles in saline,

$$\overrightarrow{F_g} - \overrightarrow{F_b} = N \cdot Vol_p(\rho_p - \rho_s)\overrightarrow{g} \qquad (1.5)$$

where $N = 25$ is the particle number in an aggregate, $Vol_p = \frac{4}{3}\pi r^3$ is the volume of a single particle, $\rho_p = 2.9500g/cm^3$ is the density of magnetic particles, $\rho_s = 1.0046g/cm^3$ the density of saline, and $\overline{\|g\|} = 9.8066m/s^2$ the acceleration due to gravity. Thus, $\| \overrightarrow{F_g} - \overrightarrow{F_b}\| = 20 \times 10^{-7}$ N.

This theoretical calculation was verified experimentally by assessing the average aggregate's velocity (20 tests) with an MRI compatible camera in a bifurcation phantom tilted at $\theta = +10°$ and $-10°$.

Theoretical Maximum Steering Angulation Against Gravity

There is a linear relationship between the magnetic force and the applied gradient.[15] The magnetic force F_m acting on a particle aggregate is

$$\boldsymbol{F_m} = NVol_p(M_p \bullet \nabla)B \qquad (1.6)$$

where $N = 25$ is the particle number in an aggregate, Vol_p is the volume (m^3) of a 200 μm (diameter) magnetic particles, $M_p = 8.85 \times 10^4$ A/m is the magnetization of the particles,

$B = 3$ T is the strength of the magnetic field, and $\nabla B = 0.0265 T/m$ is the magnetic gradient.

Thus, $F_m = 7.2 \times 10^{-7}$ N.

With a pulsatile flow (i.e. F$_s$ = 0) according to previous study,[15] we obtain

$$\sin\theta = \frac{F_t}{(F_g - F_b)} \quad (1.7)$$

and in the cross section, the rotation angles (Q$_2$) of the aggregate is, for one activated gradient,

$$\tan(Q_2) = \frac{F_{m_x}}{F_g - F_b} = \frac{F_{m_x}}{N.(\rho_p - \rho_s) \bullet Vol_p \bullet g} \quad (1.8)$$

or

$$tan(Q_2) = \frac{F_{m_x}}{(F_g - F_b) - F_{m_y}} \quad (1.9)$$

for two activated gradients where $\rho_p = 2.9500 g/cm^3$ is the density of magnetic particles, $\rho_S = 1.0046 g/cm^3$ the density of saline, and $g = 9.8066 m/s^2$ the acceleration due to gravity. Applying only one magnetic gradient at $B = 0.0265 T/m$ yields a deviation angle $Q_2 = 20.2342°$. Two activated steering gradients at $G_x = +26.5$ mT/m and $G_y = +18.0$ mT/m against the gravitational force, we can select a branch division with a positive angulation of $Q_2 = 26.1842°$ (For details see Appendix A).

Measuring the Gravitational Force

Gravitational force was measured by placing a vial containing 87 magnetic particles ($r_p = 115\mu m$ radius) in a saline solution at a distance $r = 82 \pm 3$ mm (10 tests) above a carbon steel bead ($R = 10.88$ mm) placed at the iso-center of the MR scanner. According to Maxwell's electromagnetic theory, the magnetic induction field $\overrightarrow{B}$ from a point magnetic dipole is[11]:

$$\overrightarrow{B} = \frac{\mu_0}{4\pi} \frac{3(\overrightarrow{m} \bullet \overrightarrow{r})\overrightarrow{r} - \overrightarrow{m}r^2}{r^5} \quad (2.1)$$

with $\overrightarrow{m}$ the net magnetic dipole moment producing a dipolar magnetic field, μ_0 the vacuum permeability (4π $\times 10^{-7}$ H/m) and $\overrightarrow{r}$ the position vector between the aggregate and the bead. The magnetic moment of the bead can be expressed as the volume of the magnetization field[14]:

$$\overrightarrow{m} = \overrightarrow{M} dV = \frac{4\pi R^3}{3} \overrightarrow{M} \quad (2.2)$$

with $\overrightarrow{M}$ the vector sum of magnetic dipoles, V the volume and R the radius of the bead. It follows $\|\overrightarrow{B}\| = 71.59 mT/m$ as the equivalent magnetic force in [mT/m] of the theoretical gravitational force in a 3T MRI.

The steering gradient force applied on each particle is[18]:

$$\overrightarrow{F_m} = V_p M_p \overrightarrow{G} \quad (2.3)$$

where V_p is the volume of the magnetic particles in [m^3], M_p is the constant volume of magnetization (88.5×10^3 A/m), $\overrightarrow{B}$ magnetic induction field in [N.$\frac{m}{A}$ = T], and $\overrightarrow{G}$ the magnetic gradient vector ($\overrightarrow{G} = [\frac{\partial B_z}{\partial x}; \frac{\partial B_z}{\partial y}; \frac{\partial B_z}{\partial z}]$) in [T/m] at 3T. To counteract gravity and lift off the aggregate in the solution, the steering gradient force must be:

$$\overrightarrow{F_m} \geq V_p(\rho_p - \rho_S)\overrightarrow{g} \quad (2.4)$$

with $\rho_p = 2.9500 g/cm^3$ the density of magnetic particles, $\rho_s = 1.0046 g/cm^3$ the density of the saline solution and $g = 9.8066 N/kg$ the gravitational acceleration. Thus,

$$\|\overrightarrow{G}\| \geq 71.85 mT/m$$

which is the required magnetic force in [mT/m] to lift off the aggregate in the 3T MRI, meaning that it is equivalent to the gravitational force in [mT/m]. This experimental value agrees with the theoretical value of the gravitational force (71.59 mT/m). Therefore, it is not possible to steer with 43mT/m MRI gradient the particles against the force of gravity. However, the gradients and the duty cycle can be optimized to increase the overall steering force.

Steering Gradients in the MRN Sequence

The MRN sequence is based on the Echo Planar Imaging (EPI) readout which accounts for the gradient cooling. The duty cycle is defined as:

$$dutycycle = \frac{\delta}{TR} \frac{G}{G_{max}} \quad (3.1)$$

with δ the gradient duration (ramp up + plateau) in [ms], TR the repetition time in [ms], G the applied gradient amplitude in [mT/m] and G_{max} the maximum gradient amplitude allowed (43 mT/m). Previous MRN experiments used a single gradient steering along the x (horizontal) plane orthogonal to the vessel centerline to divert aggregates to the target vessel.[15, 16, 21] However, the steering gradients in the x (i.e. G_x), y (i.e. G_y) and z (i.e. G_z) directionare defined by its nominal value as:

$$G = \sqrt{(G_x^2 + G_y^2 + G_z^2)}. \quad (3.2)$$

BMES BIOMEDICAL ENGINEERING SOCIETY
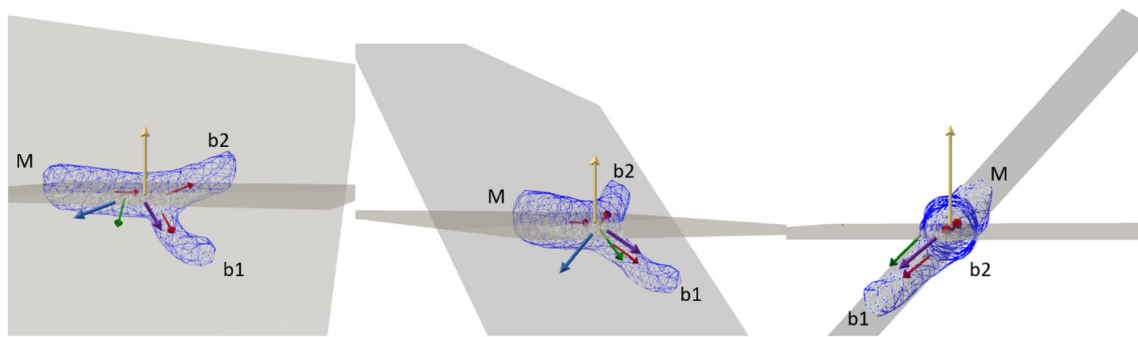
FIGURE 2. Front and side views of a segmented vascular branch. Four steering possibilities in the main hepatic artery ($\overrightarrow{M}$) to a targeted branch ($\overrightarrow{b_1}$) downward from a branch ($\overrightarrow{b_2}$), either perpendicular to the main branch (green arrow), opposite to the other non-target branch (blue arrow), parallel to the targeted branch (purple arrow) or against the gravity (yellow arrow)).

Any contributions from other axes increase the steering force. Further, applying a gradient against gravity ($+G_y$ axis) would decrease the influence of the gravitational force.

Several combinations of steering directions are possible to deviate aggregates toward a targeted branch. The steering gradient can be oriented perpendicular to the main branch to deviate the aggregates on the side of the target branch ($\perp \overrightarrow{M}$), opposing the non-target branch ($-\overrightarrow{b_2}$) to prevent the aggregate from entering the non-target branch or parallel to the targeted branch ($\parallel \overrightarrow{b_1}$). To minimize the impact of gravity and frictional forces, another gradient opposing gravity ($-\overrightarrow{g}$) can be combined with the steering gradient (Fig. 2). Steering against the non-target branch is the sum vector of decreasing the flow force, i.e. the aggregate velocity, and steering perpendicular to the main branch to deviate the aggregate toward the target branch. While steering parallel to the main branch is the vector sum of steering perpendicular to the main branch and increasing the flow force, the aggregate velocity, in the main branch. The thrust force that will drive the aggregates will be controlled by the flow downstream from the catheter which is a combination of the flow due to catheter perfusion and peripheral pulsatile flow around the balloon catheter (bypass flow). This proximal control of the flow to modify the thrust force is more important than the effect of either decreasing the gradient or decreasing velocities in the non-target or target branch.[21] The magnitude of the gravitational force is also higher than the gradient magnetic force. Thus, we tested a gradient perpendicular to the main branch and aligned in the direction of the target branch to deviate aggregates. The orientation of these branches was determined according to the averaged centerline from prior segmentations. This gradient was applied alone or in combination with a vertical gradient to elevate the aggregate.

The Experimental Setup

A compromise between gradient amplitude and duty cycle was verified experimentally by measuring the steering success rate against gravity in a single-bifurcation phantom tilted at $+15$ degree above horizontal plane. Poly-vinyl alcohol hydrogel (PVA-H), which is made of poly-vinyl alcohol (PVA) and water, is ideal for mimicking dynamic viscoelasticity and friction resistance of blood vessels.[13] The steps to prepare the PVA phantom are detailed in the Appendix B. Its transparency allows the MRI acquisitions to be compared using an MRI compatible video camera to assess flow and the MRN success, i.e. the number of times the aggregate reaches the targeted branch.

An aqueous 33% (w/v) glycerol solution was used to reproduce the viscosity of blood (2.78 mPa.s, 2.65 mm^2/s)[5]. The total flow was set at 0.6 mL/s by tuning the cardiac heart pump, manually measured by collecting the outlet flow coming from the two branches of the phantom for 20 s in a graduated beaker, and double confirmed with the flow measurement from a 2D cine phase contrast MRI sequence (MRI parameters detailed below). (see Fig. 3, for a schematic of the phantom). During the injection, a cardiac pump (Harvard Apparatus pulsatile blood pump, USA) operating at 60 bpm, with a systole/diastole duration ratio of 30/70, and a stroke volume of 16 mL provides a 0.60 mL/s flow volume while the aggregate is injected at 0.20 mL/s (Fig. 3). Details of the aggregate injector system are provided in,[15] while images of the setup are provided in the supplementary material to be able to reproduce the methodology (Appendix B).

A 5-French compliant occlusion balloon catheter (Cordis, Johnson & Johnson, NJ, USA) was placed in the main branch 5 cm away from the bifurcation to account for the turbulent flow from the jet. The balloon was partially inflated (0.6 mL water) to preserve a pulsatile flow, thus to maintain motion to minimize friction with the inner surface of the vessel as demon-
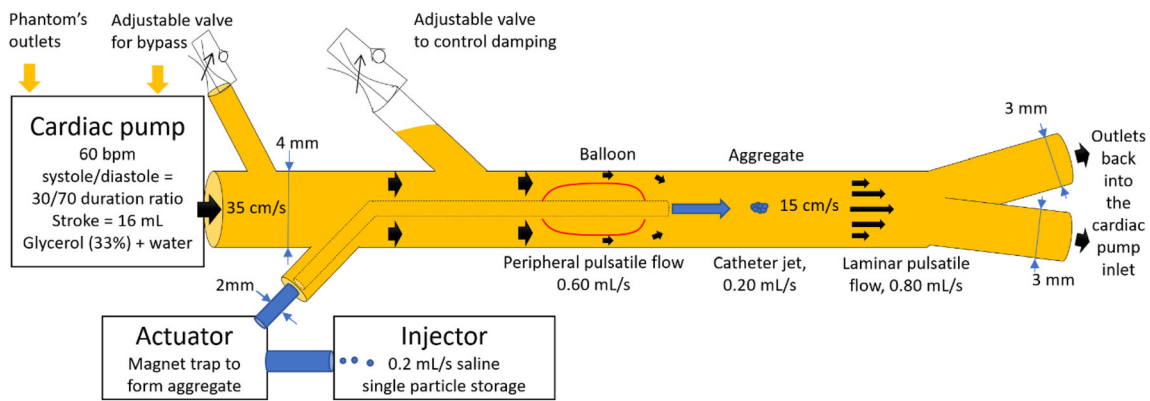
FIGURE 3. One bifurcation PVA phantom is connected to a cardiac pump with an adjustable bypass and damping to simulate in vivo flow conditions. A partially inflated catheter balloon decreases the flow velocity from 35 to 15 cm/s (systole) to control aggregate navigation while preserving a pulsatile flow to minimize friction with the inner vessel.
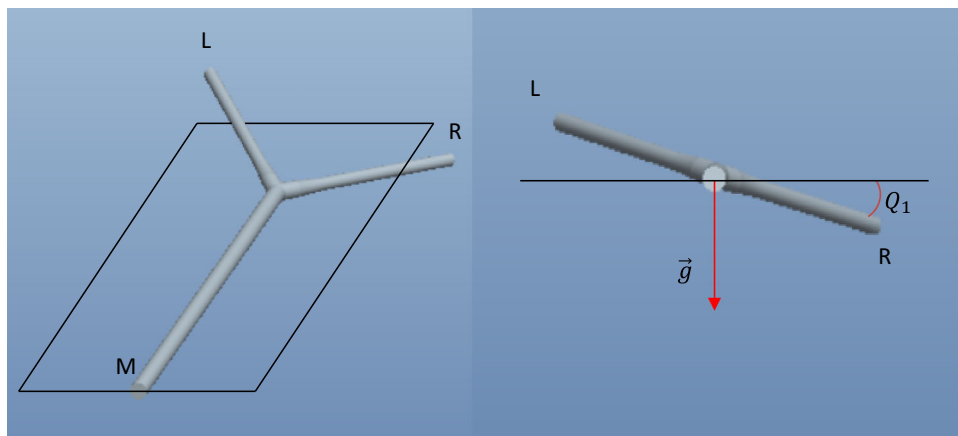
FIGURE 4. Side and front view of one bifurcation PVA phantom (M: main, L: left, R: right branches) tilted at an angle Q_1 from the horizontal plane.

strated during previous *in vitro* testing.[17] The flow becomes pulsatile and laminar beyond the jet stream to allow MRN before the bifurcation. The flow distribution in each branch division was equivalent at the baseline position (0° angulation, 0.4 mL/s in each branch) and provided 50% steering success without MRN and 100% steering success with MRN at 26.5 mT/m perpendicular to the main branch. It is important to note that contrary to other catheter brands, the Cordis catheter was used because it does not contain any ferromagnetic rings to hold the balloon which would otherwise trap the magnetic aggregate. The cardiac pump and the actuator which are not MRI compatible, were placed in the MRI control room, 5 m away from the MRI isocenter. Due to the tube's length and the difference of elevation between the MRI and the control room, the bypass and damping were adjusted to reproduce *in vivo* flow condition in the phantom.

The flow velocity was measured with a 2D cine phase-contrast sequence and a manual measurement at the inlet and outlets. The cine phase requires a cardiac trigger to encode the cardiac phase. An air pressure sensor was connected to the adjustable valve controlling the damping and the trigger placed at the beginning of the ventricular pressure wave. The cross-section of the main (4 mm) and bifurcation branches (3 mm) were acquired with cine phase contrast at TR = 78.4 ms, TE = 5.63 ms, flip angle = 20°, FOV = 128, VENC slice (z) = 60, voxel size = 0.5 mm × 0.5 mm × 4 mm in a PVA phantom placed horizontally. The flow velocity was compared with manual measurement of the flow rate at 0.5, 0.6, 0.7, 0.8 and 0.9 mL/s for two cardiac phases cycle. The flow velocity v in [cm/s] in the branches was calculated from the equation below:

$$v = \frac{Volume}{t\pi r^2} \qquad (4.1)$$

where *Volume* is the liquid volume collected from the two outlets of the two sub-branches in the time of $t = 20s$ in a graduated beaker, and r is the internal radius of the branch in [cm].

The optimized gradient combination, duty cycle and maximum steering angle against gravity were determined by tilting the phantom (Fig. 3) to an angle Q_1 (Fig. 4).

Finally the estimation of aggregate elevation due to the gravitational gradient was assessed by measuring the angle Q_2 which is the deviation angle of the aggregate from the bottom of the vessel to the lateral portion of the vessel wall (gravity direction).

RESULTS

The Optimum Duty Cycle and Gradient Strength

A series of gradient amplitudes were tested to verify their respective duty cycle (Fig. 5). The duty cycle falls because it is inversely proportional to $G_{max} = 43$ mT/m. The repetition time is 100 ms, thus at 25 mT/m the gradient is activated 49.9% of the time but its duty cycle is 29%.

Figure 6C shows that a nominal amplitude of $364.97(\text{gradient}_{nominal})^{-1.217}$ is gained, for instance a gain of 9.49mT/m at a nominal amplitude of 20 mT/m when two gradients are simultaneously activated. There is a power relationship between the duration and

the amplitude of the MRI gradient (in X: Amplitude $= 78.717 (\text{duration})^{-0.525}$, in Y: Amplitude $= 56.93 (\text{duration})^{-0.547}$).

According to preliminary results in the rheologic model, it is expected to not be possible to steer against gravity with an angle more than 23.7°. The current test is thus for an angle at 15 ° to compare the steering success of two simultaneously activated gradients versus a single one (Fig. 7)

Figure 7 shows that when the read and phase gradients ($G_x = +26.5$ mT/m, $G_y = 18$ mT/m) are simultaneously activated, the success rate in the branch tilted at $+15°$ is 87% while the success rate is only 55% with only one gradient ($G_x = +35$ mT/m). These two gradients yield a nominal amplitude of 32 mT/m at 29.45% duty cycle, meaning that gradients should be activated at about 1/3 of the time to guarantee steering success while maintaining sufficient nominal steering force. The duration of these two gradients is 8 ms. These gradient conditions will be considered as the optimal duty cycle given their steering success rate.

Steering Against Gravity Under Optimal Duty Cycle

MRN with two activated gradients is successful up to 70% at the first bifurcation with 20° angulation against the gravitational force (Fig. 8), whereas the same success rate with only one gradient is achieved with an angle between 0° and 5°. The steering success rate is a binary result, it follows with Bernoulli prob-
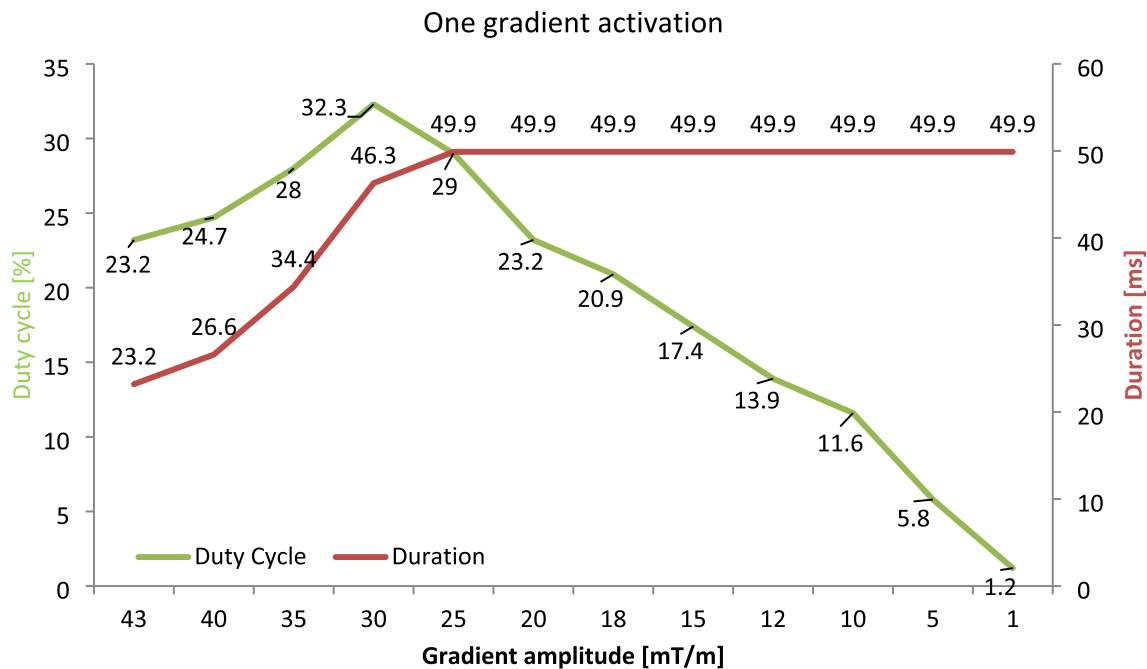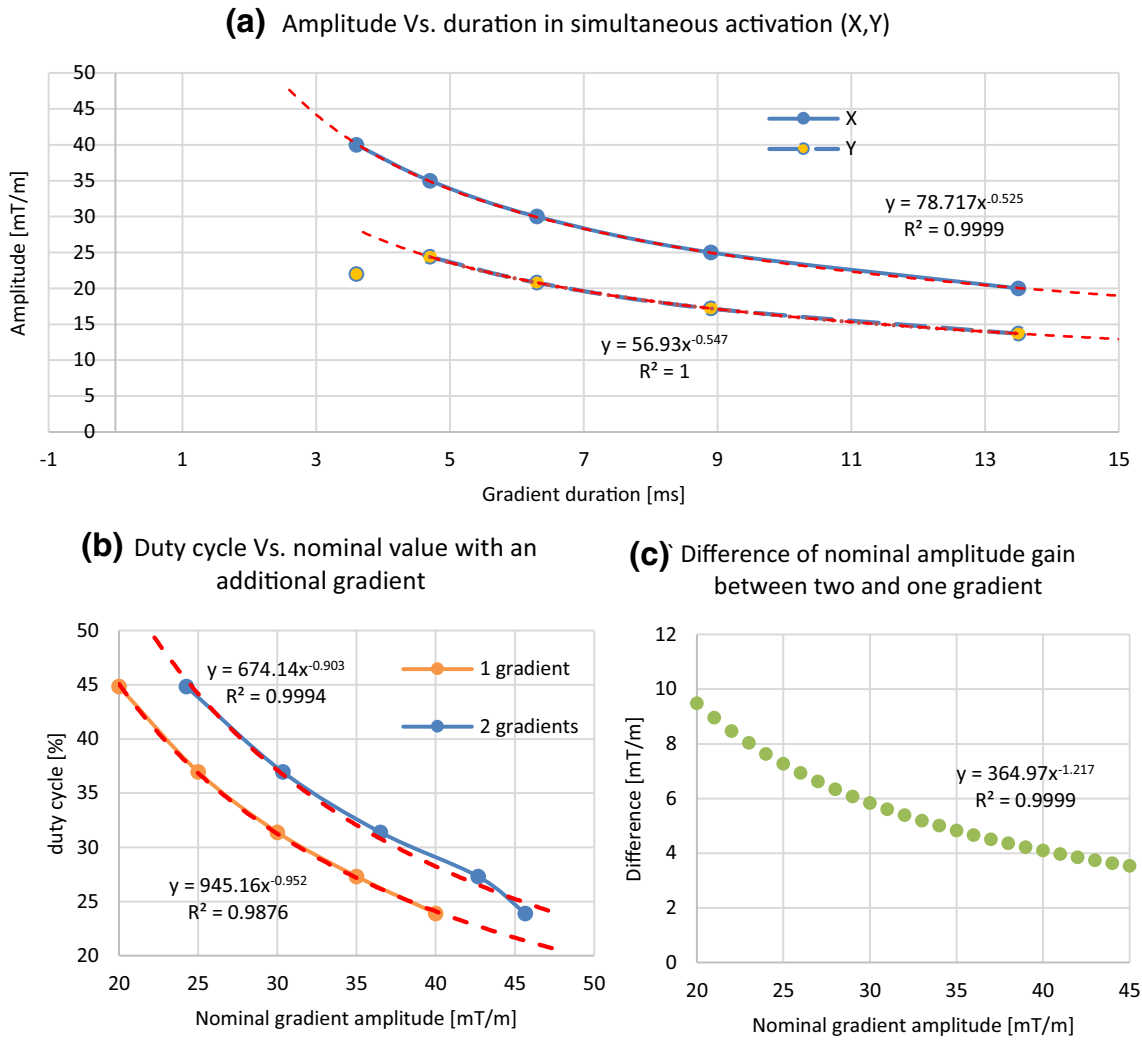

FIGURE 5. 3T MRI performance with one activated gradient, the amplitude determines the maximum duration which yields the respective duty cycle.

(a) Amplitude Vs. duration in simultaneous activation (X,Y)

(b) Duty cycle Vs. nominal value with an additional gradient

(c) Difference of nominal amplitude gain between two and one gradient

FIGURE 6. Simultaneous activation of the X and Y gradients (blue lines) with their respective amplitude, gradient duration, and duty cycle (A). In B, the duty cycle is shown according to the nominal sum of the gradients activated and their difference is displayed in C.

ability the standard error equal to the square root of the variance (Var)

$$Var = p\frac{1-p}{n} \qquad (5)$$

where p is the mean and n is the sample size ($n = 20$).

Steering Against $\overrightarrow{B0}$ Under the Optimal Duty Cycle

The aggregate orientation corresponds to the magnetic field $\overrightarrow{B0}$.[16] To test whether the form of the aggregate along $\overrightarrow{B0}$ can affect MRN steering success, the phantom was kept at 15° above the coronal plane (*XZ*) and rotated along the phase direction (Y axis) at 0°, 15°, 30°and 45°. Without steering, all the aggregates would go in the downward branch because of the gravity on the particles. Previous phantom testing without elevation provides 100% steering success along with different rotations from B0.[16] Regardless of the orientation of the phantom to $\overrightarrow{B0}$ we found no difference in the MRN success rate (Table 1). The steering was kept perpendicular to the main bifurcation for each orientation, the second gradients (G_y) (the one acting against gravity) was kept at 18 mT/m, and tested twenty times for each rotation.

Moreover, there was no difference between the MRN success rate and the variation of the heart rate from 60 bpm to 90 bpm when the phantom was tilted at +15° above the coronal plane.

Experimental Verification of the Rheologic Model

From three measurements at $Q_1 = [10°,-10°,0°]$, the mean aggregates' velocity was 1.34 ± 0.18 cm/s, 1.59 ±

Steering success rate and activated gradients
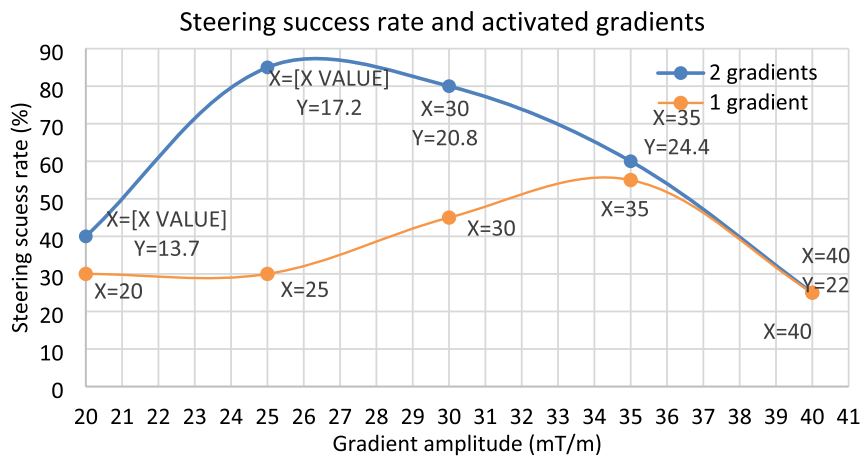
X	20	25	26.5	30	35	40
Y	13.7	17.2	18	20.8	24.4	22
nominal amplitude	24.2	30.3	32	36.5	42.7	45.7
duty cycle	37.9	31	29.5	26.2	22.7	21.4

FIGURE 7. Steering success rate against gravity in one bifurcation tilted at +15 degree along $\overrightarrow{B0}$ with one activated gradient (readout (+G_x), green) or two activated gradients (read (+G_x) and phase (+G_y), blue).
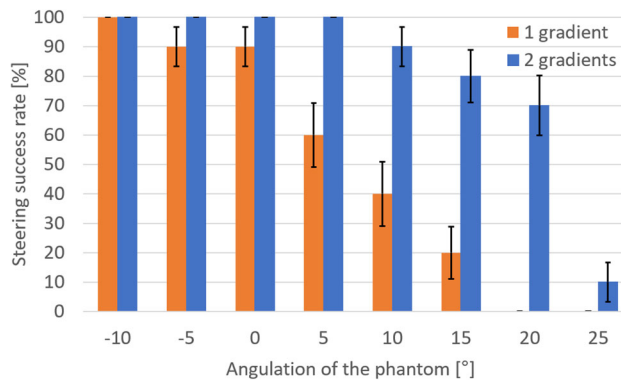
FIGURE 8. Percentage of steering success rate with two activated gradients under the optimal duty cycle (G_x = +26.5 mT/m, G_y = 18 mT/m) according to the angulation of the branch tilted against gravity in degree along $\overrightarrow{B0}$.

TABLE 1. Steering success rate in a single bifurcation phantom tilted at 15° above the coronal plane and rotated along the Y axis of the MRI while keeping steering orientation perpendicular to the main branch.

	Amplitudes			
Rotation along Y axis in degrees	X	Y	Z	Success rate [%]
0	− 26.5	18	0	60
15	− 25.2	18	7.1	50
30	− 21	18	15.3	60
45	− 18	18	18.8	50

0.14 cm/s, 1.46 ± 0.18 cm/s (mean ± SD, n = 20), respectively, using a flow velocity of 8 cm/s and an MRI compatible camera with a frame rate of 30 fps. We can retrieve V_{ba}, σ and μ

From equation (Eq 2.4) with (Eq 2.5),
$F_t = \mu \cdot (F_g - F_b) cos(0) = 10 \times 10^{-7}$ N
$V_{ba} = 1.8$ cm /s
$\sigma = 2.77 \times 10^{-4}$ N.s/m^2
$\mu = 0.5$

Thus, at $\theta = 0°$, the thrust force from the flow on the particle aggregate is 10×10^{-7} N, which is also the dynamic friction force on the particles. Although the mean flow velocity is 8 cm/s (0.8 mL/s pulsatile flow and 0.2 mL/s constant flow in a 4 mm tube) in the main branch of the PVA phantom, the flow bypassing the particle aggregate is only 1.8 cm/s. The weight of a particle aggregate is $N \cdot Vol_p \cdot \rho_p \cdot g = 30.2 \times 10^{-7}$ N which yield the gravitational force, $F_g - F_b$, at 20×10^{-7} N.

This result is consistent with our theoretical model on the thrust force. Figure 4 in Appendix B shows a video of the particle speed on the camera and the respective MR TRUFI images.

DISCUSSION

Magnetic resonance navigation (MRN) of microrobots has so far relied on either external gradients coils,[4] small animal 7T scanner,[6] Helmholtz Coil System[12] and rotating magnetic field[1] to either compensate for the lower gradients amplitude found in clinical MRI (~ 43mT/m) or to find an alternative. Our results show that MRN is still possible using a 3T clinical MRI if all the forces applied on the microrobots are considered in the navigation: friction, gravity and buoyancy forces, combined MRI gradients amplitude and thrust force from the blood flow.

For steering, the gradient duration δ and amplitude G have a power relationship ($G = 78.717 \ \delta^{-0.525}$). According to the Siemens 3T MRI Skyra design specifications, the vector sum of the three orthogonal axis is limited to 78 mT/m which is consistent with our measurement. Previous *in vitro* experiment selected 20 mT/m for half of the sequence duration which yields a duty cycle of 23.2%.[21] The simultaneous activation of the steering gradient perpendicular ($G_x = +26.5$ mT/m) to the targeted branch at $+15°$ above horizontal plane and the second gradient ($G_y = +18$ mT/m) to minimize the gravity force yields a 32 mT/m nominal amplitude in average across time to increase the success rate from 55 to 87% compared to a single gradient activation ($+G_x$). No significant difference was observed in MRN steering success when the aggregate was steered along $\overrightarrow{B0}$ or at 15°, 30° and 45° from $\overrightarrow{B0}$. The variation of heart rates from 60 to 90 bpm did not affect the MRN success, which suggests that patients with a differing resting pulse could thus undergo a successful MRN procedure.

Since the sequence is based on the Echo Planar Readout (EPI), which accounts for the gradient cooling, the MRI can sustain the nominal value for the steering duration. Steering is only required for less than 10 seconds because the aggregate velocity is ~1.5 cm/s at 8 cm/s flow velocity. The flow on MDEB aggregates inside a bifurcation aligned with the horizontal plane (no gravity favor) provides a thrust force equivalent to the aggregate's dynamic friction force. We were able to steer the aggregates when the flow was less than 10 cm/s or about 6 times the aggregate's speed. Imaging while steering had been proposed using either a large metallic bead (2 mm diameter) or by disregarding pulsatile flow and gravitational forces.[7,8,15] Their sequences were limited to one image per second which is insufficient to keep track of the microrobots moving at more than 1.5 cm/s across bifurcation branches. The measured gravitational force was found experimentally to be 71.85 mT/m, compared to 71.60 mT/m theoretically. Given the MRI gradient strength (26.5 mT/m), the steering success rate declines with higher elevation angles opposing gravity. An adequate patient positioning would take advantage of the gravitational force to target the desired bifurcations. The pathway to the tumor will consider the influence of the gravity on the aggregate trajectory.

For liver chemotherapy, if the first bifurcation of the main hepatic artery (right-left branches) is placed at zero degrees in the coronal plane with an adequate patient's position, the second bifurcation should not be oriented more than 15° above this plane to reach 80% MRN success. Reaching a second bifurcation will allow a segmental or sublobar embolization. In fact, from an atlas of 19 patients with 32 hepatocellular carcinoma nodules all the nodules ($n = 14$) in the left lobes could be reached with MRN within two bifurcations.[23] To reach the right lobes nodules ($n = 18$), three bifurcations are sufficient. Seventy-five percent of the elevation angles of the branch divisions were below the horizontal plane. There are only two cases where the bifurcation elevation angle was above 20°. Thus, only two nodules out of the 32 (6.2%) would have been rejected for MRN. To align all vascular bifurcations with minimal or no elevation relative to the horizontal plane, the patient must be situated in a prone position for left lobe nodules, supine position for right lobe nodules.

To perform such patient position *in vivo*, e.g. for liver chemotherapy, the proper hepatic artery would be catheterize in the X-ray angiography room. Blood flow velocity would be measured for each gradual inflation of the balloon catheter until a blood flow velocity compatible with MRN (<10cm/s) is reached which would inform us on the volume required for the optimal inflation of the balloon. The second step would be to bring the patient to the MRI room, where the port would be hooked up to the automatic balloon inflation device and the MDEB aggregate injector. The patient would first be scanned for anatomic and flow study

(2D phase contrast MRI for a 20 sec breath-hold or 4D flow for 6 min). With the patient placed in a position that favors gravity acting on the MDEBs, and while blood flow being controlled, the MDEB aggregates would be injected aggregate-by-aggregate until the targeted segment is embolized.

Our *in vitro* study presents several limitations. Although the temperature of the fluid was not at body level (37.5°C), the proportion of glycerol was adapted (1/3 of the volume) to obtain the viscosity of blood. Ideally, blood should be used during our experiments, but it would be more challenging to assess the steering success of the aggregates while maintaining blood temperature, oxygenation and preventing blood clots in the catheter. With the recent clinical use of 7T MRI, MRN success rate could be improved with higher magnetic field strength ($\overrightarrow{B0}$) because it will led to less particles dispersion from the aggregate.[1] The proposed rheologic model calculates the maximum steering angle that MRN can perform given the nominal amplitude of all the MRI gradients involved; this means that aggregates can be steered up to the angulation determined by the model. In our experiment, $70 \pm 10\%$ of the aggregates could be steered to a 20-degree elevated branch. At 25-degree angulation, $10 \pm 6\%$ of aggregates reach the targeted branch. Our theoretical model estimates that 26-degree angulation is the limit to steer the aggregate to the elevated branch. The difference between the theory and experiment could be due to the aggregate's shape affecting the drag force,[20] and the time of aggregate release with the cardiac cycle. A release at diastole does not have the same effect than a release at systole because the aggregate has more time to be steered to the left or right inner wall in diastole phase. One limitation of our model is that it does not calculate the steering success rate beyond the angulation limit, which was done experimentally. However, after calculating the steering angle when different MRN sequences are used, we can estimate which sequence will supply the best targeting effect for the MDEBs. One gradient can reach 43 mT/m, but in reality, has only 23.2% duty cycle. Using MRI with multiple dedicated gradients 60 mT/m or even 300 mT/m would overcome the gravitational force (~72 mT/m) to increase steering success rate regardless of the vascular angulation. Patient's positioning would therefore not be required.

In conclusion, steering MDEBs in an *in vivo* flow condition is feasible in a clinical MR scanner if two gradients are simultaneously activated and the flow velocity is minimized to 8 cm/s with a residual pulsatile flow to minimize friction force. Phantom experiments indicated that the target branch should not have a positive elevation of more than 15 degrees compared to the non-target branch. The analysis of data indicates the position in which patients will need to be positioned to perform MRN *in vivo* to account for gravitation force, steering gradient efficiency, and thrust force. This approach could be also optimized by using computational flow modeling to simulate the different forces and optimize the different parameters (patient positioning, flow control and gradient direction and timing).

SUPPLEMENTARY INFORMATION

AUTHOR CONTRIBUTIONS

GS and SL supervised the studies. CT and NL implemented the methods and analysis. All authors edited the manuscript.

DATA AND MATERIALS AVAILABILITY

All data needed to evaluate the conclusions in the paper are present in the paper or the Supplementary Materials.

CONFLICT OF INTEREST C.T is currently supported by Transmedtech and Siemens Healthineers, Canada. G.M and M.J.C work at Siemens Healthineers. The other authors declare that they have no competing financial interests.

ACKNOWLEDGMENTS

REFERENCES

[1] Abolfathi, K., M. R. H. Yazdi, and A. K. Hoshiar. Studies of different swarm modes for the MNPs under the rotating magnetic field. *IEEE Trans. Nanotechnol.* 19:849–855, 2020.

[2] Azizi, A., C. C. Tremblay, K. Gagné, and S. Martel. Using the fringe field of a clinical MRI scanner enables robotic navigation of tethered instruments in deeper vascular regions. *Sci. Robot.* 4:7342, 2019.

[3] Bigot, A., G. Soulez, and S. Martel. A prototype of injector to control and to detect the release of magnetic beads within the constraints of multibifurcation magnetic resonance navigation procedures. *Magn. Reson. Med.* 77:444–452, 2017.

[4] Bigot, A., C. Tremblay, G. Soulez, and S. Martel. Magnetic resonance navigation of a bead inside a three-bifurcation PMMA phantom using an imaging gradient coil insert. *IEEE Trans. Robot.* 30:719–727, 2014.

[5] Cheng, N.-S. Formula for the viscosity of a glycerol−water mixture. *Ind. Eng. Chem. Res.* 47:3285–3288, 2008.

[6] Erin, O., M. Boyvat, J. Lazovic, M. E. Tiryaki, and M. Sitti. Wireless MRI-powered reversible orientation-locking capsule robot. *Adv. Sci.* 2021. https://doi.org/10.1002/advs.202100463.

[7] Felfoul, O., A. T. Becker, G. Fagogenis, and P. E. Dupont. Simultaneous steering and imaging of magnetic particles using MRI toward delivery of therapeutics. *Sci. Rep.* 6:33567, 2016.

[8] Folio, D., and A. Ferreira. Two-dimensional robust magnetic resonance navigation of a ferromagnetic microrobot using pareto optimality. *IEEE Trans. Robot.* 33:583–593, 2017.

[9] Gaba, R. C., R. P. Lokken, R. M. Hickey, A. J. Lipnik, R. J. Lewandowski, R. Salem, D. B. Brown, T. G. Walker, J. E. Silberzweig, M. O. Baerlocher, A. M. Echenique, M. Midia, J. W. Mitchell, S. A. Padia, S. Ganguli, T. J. Ward, J. L. Weinstein, B. Nikolic, and S. R. Dariushnia. Society of interventional radiology standards of practice committee quality improvement guidelines for transarterial chemoembolization and embolization of hepatic malignancy. *J. Vasc. Interv. Radiol.* 28:1210–1223, 2017.

[10] Hoshiar, A. K., T.-A. Le, P. Valdastri, and J. Yoon. Swarm of magnetic nanoparticles steering in multi-bifurcation vessels under fluid flow. *J. Micro-Bio Robot.* 16:137–145, 2020.

[11] Jackson, J. D., and J. Wiley. Classical Electrodynamics Third Editionat. https://cds.cern.ch/record/490457/files/9780471309321_TOC.pdf.

[12] Jiang, J., L. Yang, and L. Zhang. Closed-loop control of a Helmholtz coil system for accurate actuation of magnetic microrobot swarms. *IEEE Robot. Autom. Lett.* 6:827–834, 2021.

[13] Kosukegawa, H., K. Mamada, K. Kuroki, L. Liu, K. Inoue, T. Hayase, and M. Ohta. Measurements of dynamic viscoelasticity of poly (vinyl alcohol) hydrogel for the development of blood vessel biomodeling*. *J. Fluid Sci. Technol.* 3:533, 2008.

[14] Latulippe, M., and S. Martel. Dipole field navigation: theory and proof of concept. *IEEE Trans. Robot.* 31:1353–1363, 2015.

[15] Li, N., Y. Jiang, R. Plantefève, F. Michaud, Z. Nosrati, C. Tremblay, K. Saatchi, U. O. Häfeli, S. Kadoury, G. Moran, F. Joly, S. Martel, and G. Soulez. Magnetic resonance navigation for targeted embolization in a two-level bifurcation phantom. *Ann. Biomed. Eng.* 47:2402–2415, 2019.

[16] Li, N., F. Michaud, Z. Nosrati, D. Loghin, C. Tremblay, R. Plantefeve, K. Saatchi, U. Hafeli, S. M. Martel, and G. Soulez. MRI-compatible injection system for magnetic microparticle embolization. *IEEE Trans. Biomed. Eng.* 2018. https://doi.org/10.1109/TBME.2018.2889000.

[17] Li, N., C. Tremblay, and S. Martel. Combining oscillating flow & clinical MRI gradients for targeted therapy. *IEEE.* 2017. https://doi.org/10.1109/MARSS.2017.8001937.

[18] Martel, S. Combining pulsed and DC gradients in a clinical MRI-based microrobotic platform to guide therapeutic magnetic agents in the vascular network. *Int. J. Adv. Robot. Syst.* 10:30, 2013.

[19] Martel, S., C. Tremblay, et al., 2006. Controlled manipulation and actuation of micro-objects with magnetotactic bacteria. aip.scitation.org, 2006. https://aip.scitation.org/doi/abs/https://doi.org/10.1063/1.2402221.

[20] Mellal, L., K. Belharet, D. Folio, and A. Ferreira. Optimal structure of particles-based superparamagnetic microrobots: application to MRI guided targeted drug therapy. *J. Nanopart. Res.* 2015. https://doi.org/10.1007/s11051-014-2733-3.

[21] Michaud, F., N. Li, R. Plantefève, Z. Nosrati, C. Tremblay, K. Saatchi, G. Moran, A. Bigot, U. O. Häfeli, S. Kadoury, A. Tang, P. Perreault, S. Martel, and G. Soulez. Selective embolization with magnetized microbeads using magnetic resonance navigation in a controlled-flow liver model. *Med. Phys.* 46:789–799, 2019.

[22] Nosrati, Z., N. Li, F. Michaud, S. Ranamukhaarachchi, S. Karagiozov, G. Soulez, S. Martel, K. Saatchi, and U. O. Häfeli. Development of a coflowing device for the size-controlled preparation of magnetic-polymeric microspheres as embolization agents in magnetic resonance navigation technology. *ACS Biomater. Sci. Eng.* 4:1092–1102, 2018.

[23] Ouedrago I. Etude de l'anatomie artérielle hépatique chez des patients a eints de CHC, pour un traitement par chimioembolisation par navigation par résonance magnétique, 2019.

[24] Peng Cao, Y., G. Duhamel, B. Ramond. Olympe, and F. Langevin. A new production method of elastic silicone carotid phantom based on MRI acquisition using rapid prototyping technique. *Annu Int Conf IEEE Eng Med Biol Soc.* 2013. https://doi.org/10.1109/EMBC.2013.6610753.

[25] Polanczyk, A., M. Podgorski, M. Polanczyk, A. Piechota-Polanczyk, C. Neumayer, and L. Stefanczyk. A Novel Patient-Specific Human Cardiovascular System Phantom (HCSP) for reconstructions of pulsatile blood hemodynamic inside abdominal aortic aneurysm. *IEEE Access.* 6:61896–61903, 2018.

[26] Polanczyk, A., M. Podgorski, M. Polanczyk, A. Piechota-Polanczyk, L. Stefanczyk, and M. Strzelecki. A novel vision-based system for quantitative analysis of abdominal aortic aneurysm deformation. *Biomed. Eng. Online.* 18:56, 2019.

[27] Pouponneau, P., G. Bringout, and S. Martel. Therapeutic magnetic microcarriers guided by magnetic resonance

navigation for enhanced liver chemoembilization: a design review. *Ann. Biomed. Eng*. 42:929–939, 2014.

[28]Pouponneau, P., J.-C. Leroux, G. Soulez, L. Gaboury, and S. Martel. Co-encapsulation of magnetic nanoparticles and doxorubicin into biodegradable microcarriers for deep tissue targeting by vascular MRI navigation. *Biomaterials*. 32:3481–3486, 2011.

[29]Suwa, M., and H. Watarai. Magnetoanalysis of micro/nanoparticles: a review. *Anal. Chim. Acta*. 690:137–147, 2011.